

First Measurement of the W Boson Mass in Run II of the Tevatron

T. Aaltonen,²³ A. Abulencia,²⁴ J. Adelman,¹³ T. Affolder,¹⁰ T. Akimoto,⁵⁵ M.G. Albrow,¹⁷ S. Amerio,⁴³
D. Amidei,³⁵ A. Anastassov,⁵² K. Anikeev,¹⁷ A. Annovi,¹⁹ J. Antos,¹⁴ M. Aoki,⁵⁵ G. Apollinari,¹⁷ T. Arisawa,⁵⁷
A. Artikov,¹⁵ W. Ashmanskas,¹⁷ A. Attal,³ A. Aurisano,⁵³ F. Azfar,⁴² P. Azzi-Bacchetta,⁴³ P. Azzurri,⁴⁶
N. Bacchetta,⁴³ W. Badgett,¹⁷ A. Barbaro-Galtieri,²⁹ V.E. Barnes,⁴⁸ B.A. Barnett,²⁵ S. Baroiant,⁷ V. Bartsch,³¹
G. Bauer,³³ P.-H. Beauchemin,³⁴ F. Bedeschi,⁴⁶ S. Behari,²⁵ G. Bellettini,⁴⁶ J. Bellinger,⁵⁹ A. Belloni,³³
D. Benjamin,¹⁶ A. Beretvas,¹⁷ J. Beringer,²⁹ T. Berry,³⁰ A. Bhatti,⁵⁰ M. Binkley,¹⁷ D. Bisello,⁴³ I. Bizjak,³¹
R.E. Blair,² C. Blocker,⁶ B. Blumenfeld,²⁵ A. Bocci,¹⁶ A. Bodek,⁴⁹ V. Boisvert,⁴⁹ G. Bolla,⁴⁸ A. Bolshov,³³
D. Bortoletto,⁴⁸ J. Boudreau,⁴⁷ A. Boveia,¹⁰ B. Brau,¹⁰ L. Brigliadori,⁵ C. Bromberg,³⁶ E. Brubaker,¹³
J. Budagov,¹⁵ H.S. Budd,⁴⁹ S. Budd,²⁴ K. Burkett,¹⁷ G. Busetto,⁴³ P. Bussey,²¹ A. Buzatu,³⁴ K. L. Byrum,²
S. Cabrera^q,¹⁶ M. Campanelli,²⁰ M. Campbell,³⁵ F. Canelli,¹⁷ A. Canepa,⁴⁵ S. Carrilloⁱ,¹⁸ D. Carlsmith,⁵⁹
R. Carosi,⁴⁶ S. Carron,³⁴ B. Casal,¹¹ M. Casarsa,⁵⁴ A. Castro,⁵ P. Catastini,⁴⁶ D. Cauz,⁵⁴ M. Cavalli-Sforza,³
A. Cerri,²⁹ L. Cerrito^m,³¹ S.H. Chang,²⁸ Y.C. Chen,¹ M. Chertok,⁷ G. Chiarelli,⁴⁶ G. Chlachidze,¹⁷ F. Chlebana,¹⁷
I. Cho,²⁸ K. Cho,²⁸ D. Chokheli,¹⁵ J.P. Chou,²² G. Choudalakis,³³ S.H. Chuang,⁵² K. Chung,¹² W.H. Chung,⁵⁹
Y.S. Chung,⁴⁹ M. Cilizjak,⁴⁶ C.I. Ciobanu,²⁴ M.A. Ciocci,⁴⁶ A. Clark,²⁰ D. Clark,⁶ M. Coca,¹⁶ G. Compostella,⁴³
M.E. Convery,⁵⁰ J. Conway,⁷ B. Cooper,³¹ K. Copic,³⁵ M. Cordelli,¹⁹ G. Cortiana,⁴³ F. Crescioli,⁴⁶
C. Cuenca Almenar^q,⁷ J. Cuevas^l,¹¹ R. Culbertson,¹⁷ J.C. Cully,³⁵ S. DaRonco,⁴³ M. Datta,¹⁷ S. D'Auria,²¹
T. Davies,²¹ D. Dagenhart,¹⁷ P. de Barbaro,⁴⁹ S. De Cecco,⁵¹ A. Deisher,²⁹ G. De Lentdecker^c,⁴⁹ G. De Lorenzo,³
M. Dell'Orso,⁴⁶ F. Delli Paoli,⁴³ L. Demortier,⁵⁰ J. Deng,¹⁶ M. Deninno,⁵ D. De Pedis,⁵¹ P.F. Derwent,¹⁷
G.P. Di Giovanni,⁴⁴ C. Dionisi,⁵¹ B. Di Ruzza,⁵⁴ J.R. Dittmann,⁴ M. D'Onofrio,³ C. Dörr,²⁶ S. Donati,⁴⁶
P. Dong,⁸ J. Donini,⁴³ T. Dorigo,⁴³ S. Dube,⁵² J. Efron,³⁹ R. Erbacher,⁷ D. Errede,²⁴ S. Errede,²⁴ R. Eusebi,¹⁷
H.C. Fang,²⁹ S. Farrington,³⁰ I. Fedorko,⁴⁶ W.T. Fedorko,¹³ R.G. Feild,⁶⁰ M. Feindt,²⁶ J.P. Fernandez,³² R. Field,¹⁸
G. Flanagan,⁴⁸ R. Forrest,⁷ S. Forrester,⁷ M. Franklin,²² J.C. Freeman,²⁹ I. Furic,¹³ M. Gallinaro,⁵⁰ J. Galyardt,¹²
J.E. Garcia,⁴⁶ F. Garberon,¹⁰ A.F. Garfinkel,⁴⁸ C. Gay,⁶⁰ H. Gerberich,²⁴ D. Gerdes,³⁵ S. Giagu,⁵¹ P. Giannetti,⁴⁶
K. Gibson,⁴⁷ J.L. Gimmell,⁴⁹ C. Ginsburg,¹⁷ N. Giokaris^a,¹⁵ M. Giordani,⁵⁴ P. Giromini,¹⁹ M. Giunta,⁴⁶
G. Giurgiu,²⁵ V. Glagolev,¹⁵ D. Glenzinski,¹⁷ M. Gold,³⁷ N. Goldschmidt,¹⁸ J. Goldstein^b,⁴² A. Golossanov,¹⁷
G. Gomez,¹¹ G. Gomez-Ceballos,³³ M. Goncharov,⁵³ O. González,³² I. Gorelov,³⁷ A.T. Goshaw,¹⁶ K. Goulianos,⁵⁰
A. Gresele,⁴³ S. Grinstein,²² C. Grosso-Pilcher,¹³ R.C. Group,¹⁷ U. Grundler,²⁴ J. Guimaraes da Costa,²²
Z. Gunay-Unalan,³⁶ C. Haber,²⁹ K. Hahn,³³ S.R. Hahn,¹⁷ E. Halkiadakis,⁵² A. Hamilton,²⁰ B.-Y. Han,⁴⁹ J.Y. Han,⁴⁹
R. Handler,⁵⁹ F. Happacher,¹⁹ K. Hara,⁵⁵ D. Hare,⁵² M. Hare,⁵⁶ S. Harper,⁴² R.F. Harr,⁵⁸ R.M. Harris,¹⁷
M. Hartz,⁴⁷ K. Hatakeyama,⁵⁰ J. Hauser,⁸ C. Hays,⁴² M. Heck,²⁶ A. Heijboer,⁴⁵ B. Heinemann,²⁹ J. Heinrich,⁴⁵
C. Henderson,³³ M. Herndon,⁵⁹ J. Heuser,²⁶ D. Hidas,¹⁶ C.S. Hill^b,¹⁰ D. Hirschbuehl,²⁶ A. Hocker,¹⁷ A. Holloway,²²
S. Hou,¹ M. Houlden,³⁰ S.-C. Hsu,⁹ B.T. Huffman,⁴² R.E. Hughes,³⁹ U. Husemann,⁶⁰ J. Huston,³⁶ J. Incandela,¹⁰
G. Introzzi,⁴⁶ M. Iori,⁵¹ A. Ivanov,⁷ B. Iyutin,³³ E. James,¹⁷ D. Jang,⁵² B. Jayatilaka,¹⁶ D. Jeans,⁵¹ E.J. Jeon,²⁸
S. Jindariani,¹⁸ W. Johnson,⁷ M. Jones,⁴⁸ K.K. Joo,²⁸ S.Y. Jun,¹² J.E. Jung,²⁸ T.R. Junk,²⁴ T. Kamon,⁵³
P.E. Karchin,⁵⁸ Y. Kato,⁴¹ Y. Kemp,²⁶ R. Kephart,¹⁷ U. Kerzel,²⁶ V. Khotilovich,⁵³ B. Kilminster,³⁹ D.H. Kim,²⁸
H.S. Kim,²⁸ J.E. Kim,²⁸ M.J. Kim,¹⁷ S.B. Kim,²⁸ S.H. Kim,⁵⁵ Y.K. Kim,¹³ N. Kimura,⁵⁵ L. Kirsch,⁶ S. Klimenko,¹⁸
M. Klute,³³ B. Knuteson,³³ B.R. Ko,¹⁶ K. Kondo,⁵⁷ D.J. Kong,²⁸ J. Konigsberg,¹⁸ A. Korytov,¹⁸ A.V. Kotwal,¹⁶
A.C. Kraan,⁴⁵ J. Kraus,²⁴ M. Kreps,²⁶ J. Kroll,⁴⁵ N. Krumnack,⁴ M. Kruse,¹⁶ V. Krutelyov,¹⁰ T. Kubo,⁵⁵
S. E. Kuhlmann,² T. Kuhr,²⁶ N.P. Kulkarni,⁵⁸ Y. Kusakabe,⁵⁷ S. Kwang,¹³ A.T. Laasanen,⁴⁸ S. Lai,³⁴ S. Lami,⁴⁶
S. Lammel,¹⁷ M. Lancaster,³¹ R.L. Lander,⁷ K. Lannon,³⁹ A. Lath,⁵² G. Latino,⁴⁶ I. Lazzizzera,⁴³ T. LeCompte,²
J. Lee,⁴⁹ J. Lee,²⁸ Y.J. Lee,²⁸ S.W. Lee^o,⁵³ R. Lefèvre,²⁰ N. Leonardo,³³ S. Leone,⁴⁶ S. Levy,¹³ J.D. Lewis,¹⁷
C. Lin,⁶⁰ C.S. Lin,¹⁷ M. Lindgren,¹⁷ E. Lipeles,⁹ T.M. Liss,²⁴ A. Lister,⁷ D.O. Litvintsev,¹⁷ T. Liu,¹⁷ N.S. Lockyer,⁴⁵
A. Loginov,⁶⁰ M. Loreti,⁴³ R.-S. Lu,¹ D. Lucchesi,⁴³ P. Lujan,²⁹ P. Lukens,¹⁷ G. Lungu,¹⁸ L. Lyons,⁴² J. Lys,²⁹
R. Lysak,¹⁴ E. Lytken,⁴⁸ P. Mack,²⁶ D. MacQueen,³⁴ R. Madrak,¹⁷ K. Maeshima,¹⁷ K. Makhoul,³³ T. Maki,²³
P. Maksimovic,²⁵ S. Malde,⁴² S. Malik³¹ G. Manca,³⁰ A. Manousakis^a,¹⁵ F. Margaroli,⁵ R. Marginean,¹⁷
C. Marino,²⁶ C.P. Marino,²⁴ A. Martin,⁶⁰ M. Martin,²⁵ V. Martin^g,²¹ M. Martínez,³ R. Martínez-Ballarín,³²
T. Maruyama,⁵⁵ P. Mastrandrea,⁵¹ T. Masubuchi,⁵⁵ H. Matsunaga,⁵⁵ M.E. Mattson,⁵⁸ R. Mazini,³⁴ P. Mazzanti,⁵
K.S. McFarland,⁴⁹ P. McIntyre,⁵³ R. McNulty^f,³⁰ A. Mehta,³⁰ P. Mehtala,²³ S. Menzemer^h,¹¹ A. Menzione,⁴⁶
P. Merkel,⁴⁸ C. Mesropian,⁵⁰ A. Messina,³⁶ T. Miao,¹⁷ N. Miladinovic,⁶ J. Miles,³³ R. Miller,³⁶ C. Mills,¹⁰
M. Milnik,²⁶ A. Mitra,¹ G. Mitselmakher,¹⁸ A. Miyamoto,²⁷ S. Moed,²⁰ N. Moggi,⁵ B. Mohr,⁸ C.S. Moon,²⁸

R. Moore,¹⁷ M. Morello,⁴⁶ P. Movilla Fernandez,²⁹ J. Mülmenstädt,²⁹ A. Mukherjee,¹⁷ Th. Muller,²⁶ R. Mumford,²⁵ P. Murat,¹⁷ M. Mussini,⁵ J. Nachtman,¹⁷ A. Nagano,⁵⁵ J. Naganoma,⁵⁷ K. Nakamura,⁵⁵ I. Nakano,⁴⁰ A. Napier,⁵⁶ V. Necula,¹⁶ C. Neu,⁴⁵ M.S. Neubauer,⁹ J. Nielsen,^{n,29} L. Nodulman,² O. Norniella,³ E. Nurse,³¹ S.H. Oh,¹⁶ Y.D. Oh,²⁸ I. Oksuzian,¹⁸ T. Okusawa,⁴¹ R. Oldeman,³⁰ R. Orava,²³ K. Osterberg,²³ C. Pagliarone,⁴⁶ E. Palencia,¹¹ V. Papadimitriou,¹⁷ A. Papaikonomou,²⁶ A.A. Paramonov,¹³ B. Parks,³⁹ S. Pashapour,³⁴ J. Patrick,¹⁷ G. Pauletta,⁵⁴ M. Paulini,¹² C. Paus,³³ D.E. Pellett,⁷ A. Penzo,⁵⁴ T.J. Phillips,¹⁶ G. Piacentino,⁴⁶ J. Piedra,⁴⁴ L. Pinera,¹⁸ K. Pitts,²⁴ C. Plager,⁸ L. Pondrom,⁵⁹ X. Portell,³ O. Poukhov,¹⁵ N. Pounder,⁴² F. Prakoshyn,¹⁵ A. Pronko,¹⁷ J. Proudfoot,² F. Ptohos^{e,19} G. Punzi,⁴⁶ J. Pursley,²⁵ J. Rademacker^{b,42} A. Rahaman,⁴⁷ V. Ramakrishnan,⁵⁹ N. Ranjan,⁴⁸ I. Redondo,³² B. Reisert,¹⁷ V. Rekovic,³⁷ P. Renton,⁴² M. Rescigno,⁵¹ S. Richter,²⁶ F. Rimondi,⁵ L. Ristori,⁴⁶ A. Robson,²¹ T. Rodrigo,¹¹ E. Rogers,²⁴ S. Rolli,⁵⁶ R. Roser,¹⁷ M. Rossi,⁵⁴ R. Rossin,¹⁰ P. Roy,³⁴ A. Ruiz,¹¹ J. Russ,¹² V. Rusu,¹³ H. Saarikko,²³ A. Safonov,⁵³ W.K. Sakumoto,⁴⁹ G. Salamanna,⁵¹ O. Saltó,³ L. Santi,⁵⁴ S. Sarkar,⁵¹ L. Sartori,⁴⁶ K. Sato,¹⁷ P. Savard,³⁴ A. Savoy-Navarro,⁴⁴ T. Scheidle,²⁶ P. Schlabach,¹⁷ E.E. Schmidt,¹⁷ M.P. Schmidt,⁶⁰ M. Schmitt,³⁸ T. Schwarz,⁷ L. Scodellaro,¹¹ A.L. Scott,¹⁰ A. Scribano,⁴⁶ F. Scuri,⁴⁶ A. Sedov,⁴⁸ S. Seidel,³⁷ Y. Seiya,⁴¹ A. Semenov,¹⁵ L. Sexton-Kennedy,¹⁷ A. Sfyrila,²⁰ S.Z. Shalhout,⁵⁸ M.D. Shapiro,²⁹ T. Shears,³⁰ P.F. Shepard,⁴⁷ D. Sherman,²² M. Shimojima^{k,55} M. Shochet,¹³ Y. Shon,⁵⁹ I. Shreyber,²⁰ A. Sidoti,⁴⁶ P. Sinervo,³⁴ A. Sisakyan,¹⁵ A.J. Slaughter,¹⁷ J. Slaunwhite,³⁹ K. Sliwa,⁵⁶ J.R. Smith,⁷ F.D. Snider,¹⁷ R. Snihur,³⁴ M. Soderberg,³⁵ A. Soha,⁷ S. Somalwar,⁵² V. Sorin,³⁶ J. Spalding,¹⁷ F. Spinella,⁴⁶ T. Spreitzer,³⁴ P. Squillacioti,⁴⁶ M. Stanitzki,⁶⁰ A. Staveris-Polykalas,⁴⁶ R. St. Denis,²¹ B. Stelzer,⁸ O. Stelzer-Chilton,⁴² D. Stentz,³⁸ J. Strologas,³⁷ D. Stuart,¹⁰ J.S. Suh,²⁸ A. Sukhanov,¹⁸ H. Sun,⁵⁶ I. Suslov,¹⁵ T. Suzuki,⁵⁵ A. Taffard^{p,24} R. Takashima,⁴⁰ Y. Takeuchi,⁵⁵ R. Tanaka,⁴⁰ M. Tecchio,³⁵ P.K. Teng,¹ K. Terashi,⁵⁰ J. Thom^{d,17} A.S. Thompson,²¹ E. Thomson,⁴⁵ P. Tipton,⁶⁰ V. Tiwari,¹² S. Tkaczyk,¹⁷ D. Toback,⁵³ S. Tokar,¹⁴ K. Tollefson,³⁶ T. Tomura,⁵⁵ D. Tonelli,⁴⁶ S. Torre,¹⁹ D. Torretta,¹⁷ S. Tourneur,⁴⁴ W. Trischuk,³⁴ S. Tsuno,⁴⁰ Y. Tu,⁴⁵ N. Turini,⁴⁶ F. Ukegawa,⁵⁵ S. Uozumi,⁵⁵ S. Vallecorsa,²⁰ N. van Remortel,²³ A. Varganov,³⁵ E. Vataga,³⁷ F. Vazquez^{i,18} G. Velev,¹⁷ C. Vellidis^{a,46} G. Veramendi,²⁴ V. Veszpremi,⁴⁸ M. Vidal,³² R. Vidal,¹⁷ I. Vila,¹¹ R. Vilar,¹¹ T. Vine,³¹ M. Vogel,³⁷ I. Vollrath,³⁴ I. Volobouev^{o,29} G. Volpi,⁴⁶ F. Würthwein,⁹ P. Wagner,⁵³ R.G. Wagner,² R.L. Wagner,¹⁷ J. Wagner,²⁶ W. Wagner,²⁶ R. Wallny,⁸ S.M. Wang,¹ A. Warburton,³⁴ D. Waters,³¹ M. Weinberger,⁵³ W.C. Wester III,¹⁷ B. Whitehouse,⁵⁶ D. Whiteson^{p,45} A.B. Wicklund,² E. Wicklund,¹⁷ G. Williams,³⁴ H.H. Williams,⁴⁵ P. Wilson,¹⁷ B.L. Winer,³⁹ P. Wittich^{d,17} S. Wolbers,¹⁷ C. Wolfe,¹³ T. Wright,³⁵ X. Wu,²⁰ S.M. Wynne,³⁰ A. Yagil,⁹ K. Yamamoto,⁴¹ J. Yamaoka,⁵² T. Yamashita,⁴⁰ C. Yang,⁶⁰ U.K. Yang^{j,13} Y.C. Yang,²⁸ W.M. Yao,²⁹ G.P. Yeh,¹⁷ J. Yoh,¹⁷ K. Yorita,¹³ T. Yoshida,⁴¹ G.B. Yu,⁴⁹ I. Yu,²⁸ S.S. Yu,¹⁷ J.C. Yun,¹⁷ L. Zanello,⁵¹ A. Zanetti,⁵⁴ I. Zaw,²² X. Zhang,²⁴ J. Zhou,⁵² and S. Zucchelli⁵

(CDF Collaboration*)

¹*Institute of Physics, Academia Sinica, Taipei, Taiwan 11529, Republic of China*

²*Argonne National Laboratory, Argonne, Illinois 60439*

³*Institut de Fisica d'Altes Energies, Universitat Autònoma de Barcelona, E-08193, Bellaterra (Barcelona), Spain*

⁴*Baylor University, Waco, Texas 76798*

⁵*Istituto Nazionale di Fisica Nucleare, University of Bologna, I-40127 Bologna, Italy*

⁶*Brandeis University, Waltham, Massachusetts 02254*

⁷*University of California, Davis, Davis, California 95616*

⁸*University of California, Los Angeles, Los Angeles, California 90024*

⁹*University of California, San Diego, La Jolla, California 92093*

¹⁰*University of California, Santa Barbara, Santa Barbara, California 93106*

¹¹*Instituto de Fisica de Cantabria, CSIC-University of Cantabria, 39005 Santander, Spain*

¹²*Carnegie Mellon University, Pittsburgh, PA 15213*

¹³*Enrico Fermi Institute, University of Chicago, Chicago, Illinois 60637*

¹⁴*Comenius University, 842 48 Bratislava, Slovakia; Institute of Experimental Physics, 040 01 Kosice, Slovakia*

¹⁵*Joint Institute for Nuclear Research, RU-141980 Dubna, Russia*

¹⁶*Duke University, Durham, North Carolina 27708*

¹⁷*Fermi National Accelerator Laboratory, Batavia, Illinois 60510*

¹⁸*University of Florida, Gainesville, Florida 32611*

¹⁹*Laboratori Nazionali di Frascati, Istituto Nazionale di Fisica Nucleare, I-00044 Frascati, Italy*

²⁰*University of Geneva, CH-1211 Geneva 4, Switzerland*

²¹*Glasgow University, Glasgow G12 8QQ, United Kingdom*

²²*Harvard University, Cambridge, Massachusetts 02138*

²³*Division of High Energy Physics, Department of Physics,*

University of Helsinki and Helsinki Institute of Physics, FIN-00014, Helsinki, Finland

²⁴*University of Illinois, Urbana, Illinois 61801*

- ²⁵The Johns Hopkins University, Baltimore, Maryland 21218
- ²⁶Institut für Experimentelle Kernphysik, Universität Karlsruhe, 76128 Karlsruhe, Germany
- ²⁷High Energy Accelerator Research Organization (KEK), Tsukuba, Ibaraki 305, Japan
- ²⁸Center for High Energy Physics: Kyungpook National University, Taegu 702-701, Korea; Seoul National University, Seoul 151-742, Korea; SungKyunKwan University, Suwon 440-746, Korea
- ²⁹Ernest Orlando Lawrence Berkeley National Laboratory, Berkeley, California 94720
- ³⁰University of Liverpool, Liverpool L69 7ZE, United Kingdom
- ³¹University College London, London WC1E 6BT, United Kingdom
- ³²Centro de Investigaciones Energeticas Medioambientales y Tecnologicas, E-28040 Madrid, Spain
- ³³Massachusetts Institute of Technology, Cambridge, Massachusetts 02139
- ³⁴Institute of Particle Physics: McGill University, Montréal, Canada H3A 2T8; and University of Toronto, Toronto, Canada M5S 1A7
- ³⁵University of Michigan, Ann Arbor, Michigan 48109
- ³⁶Michigan State University, East Lansing, Michigan 48824
- ³⁷University of New Mexico, Albuquerque, New Mexico 87131
- ³⁸Northwestern University, Evanston, Illinois 60208
- ³⁹The Ohio State University, Columbus, Ohio 43210
- ⁴⁰Okayama University, Okayama 700-8530, Japan
- ⁴¹Osaka City University, Osaka 588, Japan
- ⁴²University of Oxford, Oxford OX1 3RH, United Kingdom
- ⁴³University of Padova, Istituto Nazionale di Fisica Nucleare, Sezione di Padova-Trento, I-35131 Padova, Italy
- ⁴⁴LPNHE, Université Pierre et Marie Curie/IN2P3-CNRS, UMR7585, Paris, F-75252 France
- ⁴⁵University of Pennsylvania, Philadelphia, Pennsylvania 19104
- ⁴⁶Istituto Nazionale di Fisica Nucleare Pisa, Universities of Pisa, Siena and Scuola Normale Superiore, I-56127 Pisa, Italy
- ⁴⁷University of Pittsburgh, Pittsburgh, Pennsylvania 15260
- ⁴⁸Purdue University, West Lafayette, Indiana 47907
- ⁴⁹University of Rochester, Rochester, New York 14627
- ⁵⁰The Rockefeller University, New York, New York 10021
- ⁵¹Istituto Nazionale di Fisica Nucleare, Sezione di Roma 1, University of Rome "La Sapienza," I-00185 Roma, Italy
- ⁵²Rutgers University, Piscataway, New Jersey 08855
- ⁵³Texas A&M University, College Station, Texas 77843
- ⁵⁴Istituto Nazionale di Fisica Nucleare, University of Trieste/ Udine, Italy
- ⁵⁵University of Tsukuba, Tsukuba, Ibaraki 305, Japan
- ⁵⁶Tufts University, Medford, Massachusetts 02155
- ⁵⁷Waseda University, Tokyo 169, Japan
- ⁵⁸Wayne State University, Detroit, Michigan 48201
- ⁵⁹University of Wisconsin, Madison, Wisconsin 53706
- ⁶⁰Yale University, New Haven, Connecticut 06520

We present a measurement of the W boson mass using 200 pb^{-1} of data collected in $p\bar{p}$ collisions at $\sqrt{s} = 1.96 \text{ TeV}$ by the CDF II detector at Run II of the Fermilab Tevatron. With a sample of 63964 $W \rightarrow e\nu$ candidates and 51128 $W \rightarrow \mu\nu$ candidates, we measure $M_W = (80413 \pm 34_{\text{stat}} \pm 34_{\text{syst}} \pm 80413 \pm 48) \text{ MeV}/c^2$. This is the most precise single measurement of the W boson mass to date.

PACS numbers: 13.38.Be, 14.70.Fm, 12.15.Ji, 13.85.Qk

*With visitors from ^aUniversity of Athens, 15784 Athens, Greece, ^bUniversity of Bristol, Bristol BS8 1TL, United Kingdom, ^cUniversity Libre de Bruxelles, B-1050 Brussels, Belgium, ^dCornell University, Ithaca, NY 14853, ^eUniversity of Cyprus, Nicosia CY-1678, Cyprus, ^fUniversity College Dublin, Dublin 4, Ireland, ^gUniversity of Edinburgh, Edinburgh EH9 3JZ, United Kingdom, ^hUniversity of Heidelberg, D-69120 Heidelberg, Germany, ⁱUniversidad Iberoamericana, Mexico D.F., Mexico, ^jUniversity of Manchester, Manchester M13 9PL, England, ^kNagasaki Institute of Applied Science, Nagasaki, Japan, ^lUniversity de Oviedo, E-33007 Oviedo, Spain, ^mUniversity of London, Queen Mary Col-

The standard model (SM) invokes the Higgs mechanism of spontaneous symmetry breaking to generate mass for the W and Z bosons, which mediate the weak force. The $SU(2) \times U(1)$ symmetry of the electroweak interaction predicts the relation between the W and Z bo-

lege, London, E1 4NS, England, ⁿUniversity of California Santa Cruz, Santa Cruz, CA 95064, ^oTexas Tech University, Lubbock, TX 79409, ^pUniversity of California, Irvine, Irvine, CA 92697, ^qIFIC(CSIC-Universitat de Valencia), 46071 Valencia, Spain.

son masses and the electromagnetic and weak gauge couplings. The prediction for the W boson mass M_W in terms of the precisely measured Z boson mass M_Z , the Fermi decay constant G_F extracted from the muon lifetime measurement, and the electromagnetic coupling α at the scale M_Z , is given in the “on-shell” scheme by [1]

$$M_W^2 = \frac{\hbar^3}{c} \frac{\pi\alpha}{\sqrt{2}G_F} \frac{1}{(1 - c_W^2)(1 - \Delta r)} \quad ,$$

where $c_W = M_W/M_Z$ and Δr is the quantum-loop correction. A precise measurement of M_W provides a measurement of Δr . In the SM the contributions to Δr are dominated by the top quark and the Higgs boson loops, such that M_W in conjunction with the top quark mass constrains the mass m_H of the undiscovered Higgs boson. An m_H constraint inconsistent with direct searches can indicate the presence of new physics, such as contributions to Δr from supersymmetric particles [2].

The W boson mass [1] has been measured most precisely by the LEP [3, 4] and Tevatron [5] experiments, with the world-average $M_W = (80392 \pm 29) \text{ MeV}/c^2$ [4]. At the Tevatron, W bosons are mainly produced in quark (q') anti-quark (\bar{q}) annihilation $q'\bar{q} \rightarrow W + X$. Here X includes the QCD radiation that forms the “hadronic recoil” balancing the boson’s transverse momentum p_T [6]. The $W \rightarrow \ell\nu$ decays, characterized by a high- p_T charged lepton ($\ell = e$ or μ) and neutrino, can be selected with high purity and provide precise mass information.

This analysis [7, 8] uses 200 pb^{-1} collected by the CDF II detector [7] in $p\bar{p}$ collisions at $\sqrt{s} = 1.96 \text{ TeV}$ at the Tevatron. CDF II is a magnetic spectrometer surrounded by calorimeters and muon detectors. We use the central drift chamber (COT) [9], the central calorimeter [10] with embedded wire chambers [11] at the electromagnetic (EM) shower maximum, and the muon detectors [12] for identification of muons and electrons with $|\eta| < 1$ [6] and measurement of their four-momenta. The muon (electron) trigger requires a COT track with $p_T > 18(9) \text{ GeV}/c$ [6], and matching muon chamber hits (EM calorimeter cluster with $E_T > 18 \text{ GeV}$).

In the analysis, we select muons with a COT track matched to muon chamber hits and passing quality requirements, track $p_T > 30 \text{ GeV}/c$, and a minimum-ionization signal in the calorimeter. Cosmic rays are rejected using COT hit timing [13]. We select electrons with track $p_T > 18 \text{ GeV}/c$, EM cluster $E_T > 30 \text{ GeV}$ [6, 7], and passing quality requirements on the COT track and the track-cluster matching. Additional requirements are based on the ratio of the calorimeter energy E to track momentum p ($E/pc < 2$), the ratio of energies detected in the hadronic and EM calorimeters $E_{Had}/E_{EM} < 0.1$, and the transverse shower profile [7]. A veto on the presence of a second lepton suppresses Z boson background, with negligible loss of W boson events. Control samples of Z boson events require two oppositely charged leptons with the above criteria.

The \vec{p}_T of the hadronic recoil (\vec{u}) equals the vector sum $\vec{u} = \sum_i E_i \sin(\theta_i) \hat{n}_i / c$ over calorimeter towers [10],

with energy E_i , polar angle θ_i , and transverse directions specified by unit vectors \hat{n}_i . Energy associated with the charged lepton(s) is not included. We impose \vec{p}_T balance to infer the neutrino’s transverse momentum $p_T^\nu \equiv |-\vec{p}_T^\ell - \vec{u}|$ [6] and the W transverse mass $m_T = \sqrt{2 (p_T^\ell p_T^\nu - \vec{p}_T^\ell \cdot \vec{p}_T^\nu)}/c$. We require $p_T^\nu > 30 \text{ GeV}/c$ and $|\vec{u}| < 15 \text{ GeV}/c$ to obtain a W candidate sample of high purity, whose m_T and lepton p_T distributions are strongly correlated with M_W . The sample consists of 63964 $W \rightarrow e\nu$ and 51128 $W \rightarrow \mu\nu$ candidates.

The W boson mass is extracted by performing binned maximum likelihood fits to the distributions of m_T , p_T^ℓ and p_T^ν . We generate 800 templates as functions of M_W between 80 GeV/c^2 and 81 GeV/c^2 using a custom Monte Carlo (MC) simulation [7] of boson production and decay, and of the detector response to the lepton(s) and hadronic recoil. The custom MC optimizes computing speed and control of systematic uncertainties. The kinematics of W and Z boson decays are obtained from the RESBOS [14] program. We tune the non-perturbative form factor in RESBOS, which describes the boson p_T spectrum at low p_T , on the dilepton p_T distributions in the Z boson data. Single photons (FSR) radiated from the final-state leptons are generated according to the WGRAD program [15]. The FSR photon energies are increased by 10% (with an absolute uncertainty of 5%) to account for additional energy loss due to two-photon radiation [16]. WGRAD is also used to estimate the initial-state QED radiation. We use the CTEQ6M [17] set of parton distribution functions and their uncertainties.

The custom MC performs a hit-level simulation of the lepton track. A fine-grained model of passive material properties is used to calculate ionization and radiative energy loss and multiple Coulomb scattering. Bremsstrahlung photons and conversion electrons are generated and propagated to the calorimeter. COT hits are generated according to the resolution ($\approx 150 \mu\text{m}$) and efficiencies measured from muon tracks in Υ, W , and Z boson decays. A helix fit (with optional beam constraint) is performed to simulate the reconstructed track.

The alignment of the COT is performed using a high-purity sample of high- p_T cosmic ray muons. Each muon’s complete trajectory is fit to a single helix [13]. The fits determine the relative locations of the sense wires, including gravitational and electrostatic displacements, with a precision of a few microns. We constrain remaining misalignments, which cause a bias in the track curvature, by comparing $\langle E/pc \rangle$ for electrons and positrons.

The tracker momentum scale is measured by template-fitting the $J/\psi \rightarrow \mu\mu$ and $\Upsilon \rightarrow \mu\mu$ mass peaks. The J/ψ fits are performed in bins of $\langle 1/p_T^\ell(\mu) \rangle$ to measure any non-linearity due to mismodelling of the ionization energy loss and other smaller effects, and in bins of $\langle \cot\theta(\mu) \rangle$ to measure the magnetic field non-uniformity. To account for the observed momentum non-linearity, a downward 6% correction to the predicted ionization energy loss is applied in the simula-

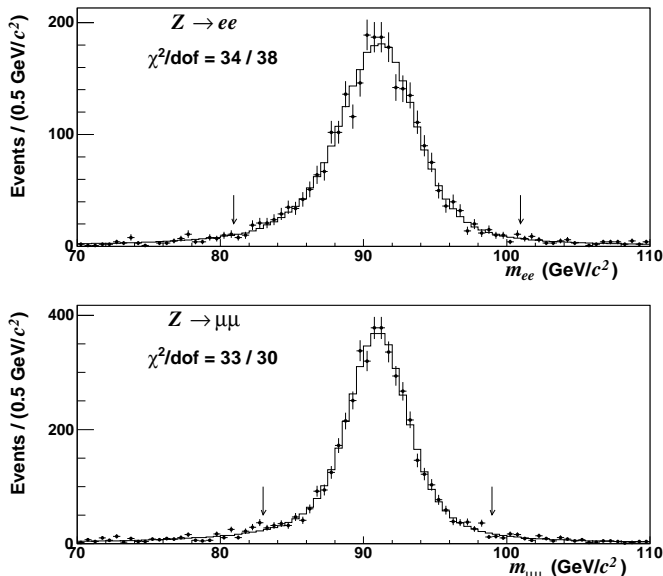


FIG. 1: The $Z \rightarrow \mu\mu$ (top) and $Z \rightarrow ee$ (bottom) mass fits, showing the data (points) and the simulation (histogram). The arrows indicate the fitting range.

tion to make the measured J/ψ mass independent of $\langle 1/p_T^\ell(\mu) \rangle$. The calibration derived from the J/ψ and Υ data yields $M_Z = (91184 \pm 43_{\text{stat}})$ MeV/ c^2 (Fig. 1) from the $Z \rightarrow \mu\mu$ data, consistent with the world average [1, 4] of (91188 ± 2) MeV/ c^2 . The systematic uncertainties due to QED radiative corrections and magnetic field non-uniformity dominate the total uncertainty of 0.02% on the combined momentum scale, derived from the J/ψ , Υ and Z boson mass fits.

We simulate the electron cluster by merging the energies of the primary electron and the proximate bremsstrahlung photons and conversion electrons. The distributions of electron and photon energy loss in the solenoid coil, and leakage into the hadronic calorimeter, are determined using GEANT [18] as a function of E_T . The fractional energy resolution is given by the quadrature sum of a sampling term ($13.5\%/\sqrt{E_T/\text{GeV}}$) and a constant term $\kappa = (0.89 \pm 0.15)\%$ applied to the cluster energy, and an additional constant term $\kappa_\gamma = (8.3 \pm 2.2)\%$ applied only to the energies of bremsstrahlung photons and conversion electrons. The κ_γ term contributes $\approx 1.3\%$ in quadrature to the effective constant term for the inclusive electron sample. The distribution of the underlying event energy [7] in the cluster is simulated. We tune κ on the width of the E/pc peak (Fig. 2) of the W boson sample, and κ_γ on the width of the $Z \rightarrow ee$ mass peak when both electrons are radiative ($E/pc > 1.06$).

Given the tracker momentum calibration, we fit the E/pc peak in bins of electron E_T to determine the electron energy scale and non-linearity. The position of the E/pc peak is sensitive to the number of radiation lengths X_0 ($\approx 19\%$), due to bremsstrahlung upstream of the COT. We constrain X_0 by comparing the fraction of

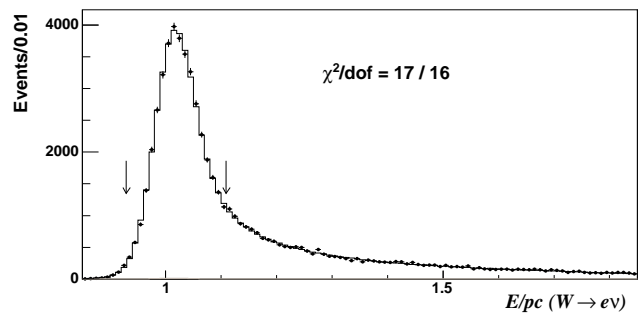


FIG. 2: The distribution of E/pc for the $W \rightarrow e\nu$ data (points) and the best-fit simulation (histogram) including the small jet background (shaded). The arrows indicate the fitting range used for the electron energy calibration. The jet background, which is barely visible on this scale, contributes a negligible uncertainty in the calibrations of the electron energy scale and the amount of radiative material.

electrons with high E/pc between data and simulation. Applying the E/pc -based energy calibration, we fit the $Z \rightarrow ee$ mass peak and measure $M_Z = (91190 \pm 67_{\text{stat}})$ MeV/ c^2 (Fig. 1), consistent with the world average [1, 4]. For maximum precision, the energy scales from the W E/pc fit and the $Z \rightarrow ee$ mass fit are combined using the Best Linear Unbiased Estimate (BLUE) method [19], with a resulting uncertainty that is mostly statistical.

The recoil \vec{u} excludes towers in which the lepton(s) deposit energy. The underlying event energy in these towers is measured from the nearby towers in W boson data, including its dependence on η^ℓ and \vec{u} . The resolution of \vec{u} has jet-like and underlying event components, with the latter modelled using data triggered on inelastic $\bar{p}p$ interactions. The recoil parameterizations are tuned on the mean and r.m.s. of the \vec{p}_T imbalance between the dilepton \vec{p}_T and \vec{u} in $Z \rightarrow \ell\ell$ events. The lepton identification efficiency is measured as a function of $u_{||} = \vec{u} \cdot \vec{p}_T^\ell / p_T^\ell$

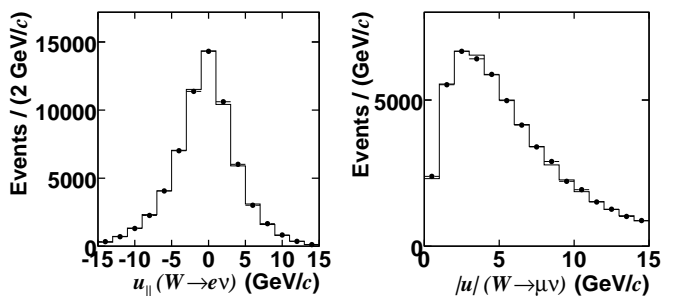


FIG. 3: Left: The $u_{||}$ distribution for the electron channel data (points) and simulation (histogram). Right: The $|\vec{u}|$ distribution for the muon channel. The mean and r.m.s. of the histograms agree between data and simulation, within the statistical precisions of $\approx 1\%$.

using the $Z \rightarrow \ell\ell$ data, in order to model its effect on the p_T^ℓ and p_T^ν distributions. Cross-checks of the recoil model using the W boson data show good agreement (Fig. 3).

| Distribution | W boson mass (MeV/ c^2) | χ^2/dof |
|-----------------|---|---------------------|
| $m_T(e, \nu)$ | $80493 \pm 48_{\text{stat}} \pm 39_{\text{syst}}$ | 86/48 |
| $p_T^\ell(e)$ | $80451 \pm 58_{\text{stat}} \pm 45_{\text{syst}}$ | 63/62 |
| $p_T^\nu(e)$ | $80473 \pm 57_{\text{stat}} \pm 54_{\text{syst}}$ | 63/62 |
| $m_T(\mu, \nu)$ | $80349 \pm 54_{\text{stat}} \pm 27_{\text{syst}}$ | 59/48 |
| $p_T^\ell(\mu)$ | $80321 \pm 66_{\text{stat}} \pm 40_{\text{syst}}$ | 72/62 |
| $p_T^\nu(\mu)$ | $80396 \pm 66_{\text{stat}} \pm 46_{\text{syst}}$ | 44/62 |

TABLE I: Fit results and uncertainties for M_W . The fit windows are 65–90 GeV/ c^2 for the m_T fit and 32–48 GeV/ c for the p_T^ℓ and p_T^ν fits. The χ^2 of the fit is computed using the expected statistical errors on the data points.

Backgrounds in the W boson candidate samples arise from misidentified jets containing high- p_T tracks and EM clusters, $Z \rightarrow \ell\ell$ where a lepton is not reconstructed and mimics a neutrino, $W \rightarrow \tau\nu$, π/K decays in flight (DIF), and cosmic rays. Jet, DIF, and cosmic ray backgrounds are estimated from the data to be less than 0.5% combined. The $W \rightarrow \tau\nu$ background is 0.9% (0.9%), and the $Z \rightarrow \ell\ell$ background is 6.6% (0.24%) in the muon (electron) channel, as estimated using a detailed GEANT-based detector simulation. The background shapes are obtained using simulation and data-derived distributions.

| Systematic | $W \rightarrow e\nu$ | $W \rightarrow \mu\nu$ | Common |
|--------------------------|----------------------|------------------------|--------|
| $p_T(W)$ model | 3 | 3 | 3 |
| QED radiation | 11 | 12 | 11 |
| Parton distributions | 11 | 11 | 11 |
| Lepton energy scale | 30 | 17 | 17 |
| Lepton energy resolution | 9 | 3 | 0 |
| Recoil energy scale | 9 | 9 | 9 |
| Recoil energy resolution | 7 | 7 | 7 |
| $u_{ }$ efficiency | 3 | 1 | 0 |
| Lepton removal | 8 | 5 | 5 |
| Backgrounds | 8 | 9 | 0 |
| Total systematic | 39 | 27 | 26 |
| Total uncertainty | 62 | 60 | 26 |

TABLE II: Systematic and total uncertainties in MeV/ c^2 for the m_T fits, which are the most precise. The last column shows the correlated uncertainties.

Table I shows the fit results from the m_T (Fig. 4), p_T^ℓ , and p_T^ν distributions. These fits are partially uncorrelated and have different systematic uncertainties, thus providing an important cross-check. The fit values were hidden during analysis by adding an unknown offset in the range [-100, 100] MeV/ c^2 . The systematic uncertainties (Table II) were evaluated by fitting MC events to propagate the analysis parameter uncertainties to M_W .

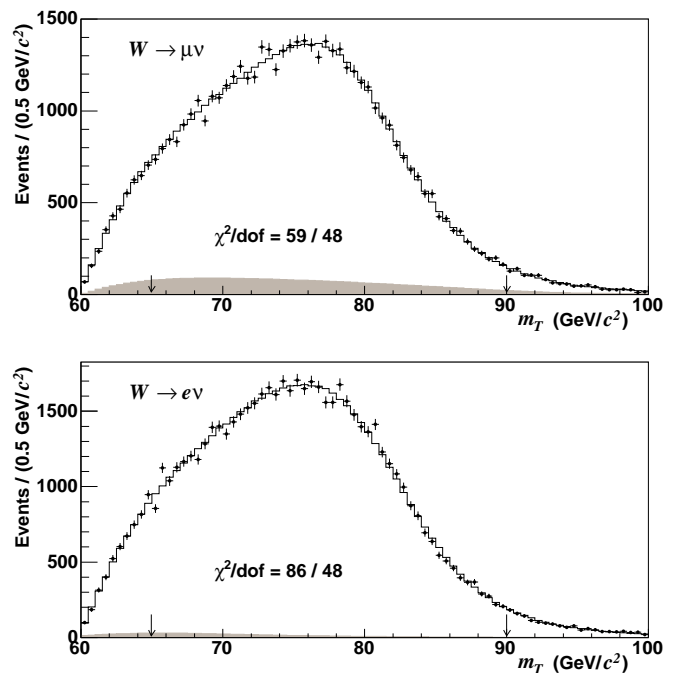


FIG. 4: The m_T distribution of the data (points) and the best-fit simulation template (histogram) including backgrounds (shaded), for muons (top) and electrons (bottom). The arrows indicate the fitting range. The χ^2/dof for the electron channel distribution receives large contributions from a few bins near 65 GeV/ c^2 , which do not bias the mass fit.

The consistency of the fit results (Table I) obtained from the different distributions shows that the W boson production, decay, and the hadronic recoil are well-modeled. The statistical correlations (evaluated using ensembles of MC events) between the m_T and p_T^ℓ (p_T^ν) fit values is 69% (68%), and between the p_T^ℓ and p_T^ν fit values is 27%. We numerically combine (using the BLUE method) the six individually fitted M_W values, including their correlations, to obtain $M_W = (80413 \pm 34_{\text{stat}} \pm 34_{\text{syst}})$ MeV/ c^2 , with $\chi^2/\text{dof} = 4.8/5$. The m_T , p_T^ℓ and p_T^ν fits in the electron (muon) channel contribute weights of 32.3% (47.7%), 8.9% (3.4%) and 6.8% (0.9%) respectively. This establishes an *a-priori* procedure to incorporate the information from individual fits. The muon (electron) channel alone yields $M_W = (80352 \pm 60)$ MeV/ c^2 ($M_W = (80477 \pm 62)$ MeV/ c^2) with $\chi^2/\text{dof} = 1.4/2$ (0.8/2). The m_T (p_T^ℓ , p_T^ν) fit results from the muon and electron channels are consistent with a probability of 7% (18%, 43%), taking into account their correlations.

In conclusion, we report the first measurement of the W boson mass from Run II of the Tevatron. We measure $M_W = (80413 \pm 48)$ MeV/ c^2 , the most precise single measurement to date, and we update the world average [4] to $M_W = (80398 \pm 25)$ MeV/ c^2 . This analysis significantly improves in precision over previous Tevatron measurements, not only through the increased integrated

luminosity but also through improved analysis techniques and understanding of systematic uncertainties. As many simulation parameters are constrained by data control samples, their uncertainties are statistical in nature and are expected to be reduced with more data. Inclusion of our result in the global electroweak fit [4, 7] reduces the predicted mass of the SM Higgs boson by 6 GeV/ c^2 and decreases its range to $m_H = 76_{-24}^{+33}$ GeV/ c^2 .

We thank the Fermilab staff and the technical staffs of the participating institutions for their vital contributions. This work was supported by the U.S. Department of Energy and National Science Foundation; the Italian Istituto Nazionale di Fisica Nucleare; the Ministry of Education, Culture, Sports, Science and Technology of Japan;

the Natural Sciences and Engineering Research Council of Canada; the National Science Council of the Republic of China; the Swiss National Science Foundation; the A.P. Sloan Foundation; the Bundesministerium für Bildung und Forschung, Germany; the Korean Science and Engineering Foundation and the Korean Research Foundation; the Science and Technology Facilities Council and the Royal Society, UK; the Institut National de Physique Nucleaire et Physique des Particules/CNRS; the Russian Foundation for Basic Research; the Comisión Interministerial de Ciencia y Tecnología, Spain; the European Community's Human Potential Programme; the European Commission under the Marie Curie Programme; the Slovak R&D Agency; and the Academy of Finland.

-
- [1] W.-M. Yao *et al.*, J. Phys. G **33**, 1 (2006).
 [2] S. Heinemeyer *et al.*, J. High Energy Phys. **0608**, 052 (2006).
 [3] S. Schael *et al.* (ALEPH Collaboration), Eur. Phys. J. C **47**, 309 (2006); G. Abbiendi *et al.* (OPAL Collaboration), Eur. Phys. J. C **45**, 307 (2006); P. Achard *et al.* (L3 Collaboration), Eur. Phys. J. C **45**, 569 (2006); J. Abdallah *et al.* (DELPHI Collaboration), to be submitted to Eur. Phys. J. C.
 [4] LEP Collaborations and LEP Electroweak Working Group, CERN-PH-EP/2006-042, and references therein.
 [5] T. Affolder *et al.* (CDF Collaboration), Phys. Rev. D **64**, 052001 (2001); V. M. Abazov *et al.* (DØ Collaboration), Phys. Rev. D **66**, 012001 (2002); B. Abbott *et al.* (DØ Collaboration), Phys. Rev. D **62**, 092006 (2000); B. Abbott *et al.* (DØ Collaboration), Phys. Rev. D **58**, 092003 (1998); V. M. Abazov *et al.* (CDF and DØ Collaborations), Phys. Rev. D **70**, 092008 (2004).
 [6] Pseudorapidity is defined as $\eta = -\ln[\tan(\theta/2)]$, where θ is the polar angle from the beam axis. Energy (momentum) transverse to the beam is denoted as E_T (p_T).
 [7] T. Aaltonen *et al.* (CDF Collaboration), submitted for publication in Phys. Rev. D; hep-ex/0708.3642.
 [8] O. Stelzer-Chilton, Ph.D. thesis, University of Toronto, 2005; I. Vollrath, Ph.D. thesis, *ibid*, 2006.
 [9] T. Affolder *et al.*, Nucl. Instrum. Methods Phys. Res. A **526**, 249 (2004).
 [10] F. Abe *et al.* (CDF Collaboration), Nucl. Instrum. Methods Phys. Res. A **271**, 387 (1988).
 [11] A. Byon-Wagner *et al.*, IEEE Trans. Nucl. Sci. **49**, 2567 (2002).
 [12] G. Ascoli *et al.*, Nucl. Instrum. Methods Phys. Res. A **268**, 33 (1988).
 [13] A. V. Kotwal, H. K. Gerberich, and C. Hays, Nucl. Instrum. Methods Phys. Res. A **506**, 110 (2003).
 [14] C. Balazs and C.-P. Yuan, Phys. Rev. D **56**, 5558 (1997); G. A. Ladinsky and C.-P. Yuan, Phys. Rev. D **50**, R4239 (1994); F. Landry, R. Brock, P. M. Nadolsky and C.-P. Yuan, Phys. Rev. D **67**, 073016 (2003).
 [15] U. Baur, S. Keller, and D. Wackerroth, Phys. Rev. D **59**, 013002 (1998).
 [16] C.M. Carloni Calame, G. Montagna, O. Nicrosini, and M. Treccani, Phys. Rev. D. **69**, 037301 (2004).
 [17] J. Pumplin *et al.*, J. High Energy Phys. **0207**, 012 (2002).
 [18] R. Brun and F. Carminati, CERN Program Library Long Writeup, W5013, 1993 (unpublished), version 3.15.
 [19] L. Lyons, D. Gibaut, and P. Clifford, Nucl. Instrum. Methods Phys. Res. A **270**, 110 (1988).